Conference Paper, Published Version

Toda, Yuji; Tsujimoto, Tetsuro; Tadakuma, Yuki

Numerical Simulation of Primary Production of Periphyton in a Sand River

NUMERICAL SIMULATION OF PRIMARY PRODUCTION OF PERIPHYTON IN A SAND RIVER

Yuji Toda[1], Tetsuro Tsujimoto[2] and Yuki Tadakuma[3]

[1] Associate Professor, Department of Civil Engineering, Nagoya University
Furo-cho, Chikusa-ku, Nagoya, 464-8603, Japan, e-mail: ytoda@cc.nagoya-u.ac.jp
[2] Professor, Department of Civil Engineering, Nagoya University
Furo-cho, Chikusa-ku, Nagoya, 464-8603, Japan, e-mail: ttsujimoto@genv.nagoya-u.ac.jp
[3] CIT Engineering, Co., Ltd.

ABSTRACT

Periphyton is known to be one of major primary producers in river ecosystem. While the growth of periphyton is usually seen on the relatively stable substrata in flowing water such as stone surface of gravel bed streams, large growth of periphyton is sometimes observed in sand river where the flow discharge and water depth are small enough for providing stable habitats for periphyton. In the present study, a numerical simulation model was presented to describe the spatial distribution of periphyton biomass at a sand river. The present numerical simulation model can predict the spatial distribution of periphyton well. A series of numerical simulation was performed to identify the effects of river discharge on the primary production of periphyton in the sand river, and the results of the simulation show that the time averaged periphyton biomass increases with the flood interval, and the net primary production of periphyton takes a peak values at the flood interval ranging about 8 to 16 days.

Keywords: Periphyton, sand river, primary production, logistic equation, flood intervals

1. INTRODUCTION

Periphyton is known to be one of major primary producers for river ecosystem, and it develops bio-film type communities on solid surface in water (MacIntire (1973), Minshall (1978), Saravia et al. (1998)). In natural streams, the periphyton communities are usually seen on the surface of gravel stones of shallow river bed and/or on the surface of submerged structures. The growth of periphyton is expected to be rarely observed in sand river reach because of high mobility of bed materials and shortage of solar illumination at the vicinity of river bed due to relatively large water depth compared with gravel reach. Nevertheless, the large growth of periphyton is sometimes seen even in sand rivers where river discharge and water depth are small enough to provide the stable habitats for periphyton.

As for rivers running through agricultural area, river water is often diverted to the agricultural fields for irrigation use, which reduces and stabilizes river discharge during ordinary water stage. This decreased and stabilized river discharge may induce the stabilization of bed materials and the resulting large growth of periphyton even on sand bed. In order to understand the base of river ecosystems in sand rivers, it is important to know the growth characteristics of periphyton on sand bed.

In the present study, a numerical simulation model was proposed to evaluate the growth characteristics of periphyton in a sand river, and the series of numerical simulation was performed to know the effects of river discharge on periphyton biomass and primary production.

2. NUMERICAL SIMULATION MODEL

Flow chart of the present numerical simulation is illustrated in figure 1, which consists of the analysis of frequency of bed material movements and the simulation of growth of periphyton during the period that the bed material sands had been at rest. In the computation of frequency of bed material movements, Shields stress on river bed τ_* was estimated by calculating by using shallow water equations on the bed geometry at a sand river. The critical Sheilds stress τ_{*c} was calculated by using Iwagaki formula (Iwagaki (1956)). Comparing between τ_* and τ_{*c}, the amount of periphyton M was estimated to 0 during the period of $\tau_*>\tau_{*c}$, and it was calculated by the numerical integration of the logistic equation during the period of $\tau_*<\tau_{*c}$.

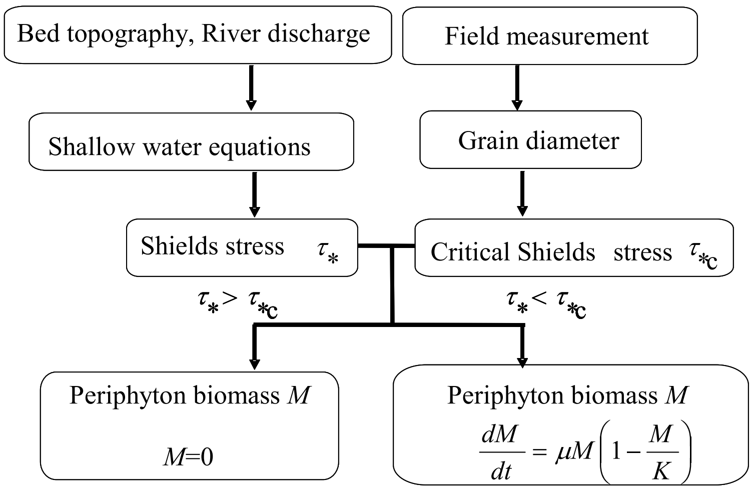

Figure 1 Flowchart of the present numerical simulation

2.1 Flow modeling

The depth-averaged continuity equation and the depth-averaged Reynolds equations in curvilinear coordinates were used for calculating horizontal flow field. Eddy viscosity was estimated by using 0-equation type turbulence closure. The governing equations for flow field were solved by finite volume method on a staggered grids system. Crank-Nicholson scheme was used for time integration. The 3rd order upwind scheme was employed for advection terms, and the 2nd order central difference was used for the other spatial derivatives.

2.2 Modeling of growth of periphyton

The logistic equation, Eq. (1), was used for the governing equation for periphyton growth:

$$\frac{dM}{dt}=\mu M\left(1-\frac{M}{K}\right) \tag{1}$$

in which M is periphyton biomass per unit area, μ is specific growth rate of periphyton and K is environmental capacity. It is expected that the parameters μ and K are the functions of the environmental conditions relating the periphyton growth. In the present simulation model, the specific growth rate μ was assumed be a function of solar radiation, water temperature and nutrient concentration. The environmental capacity K was represented by a function of solar radiation at bed surface;

$$\mu = \mu_{\max} f_I(I_b) f_T(T) f_N(N) \tag{2}$$

$$K = K_{\max} g_I(I_{b0}) \tag{3}$$

in which $\mu_{\max}$ is maximum specific growth rate, I_b is daily-averaged solar radiation at river bed, T is water temperature, N is nutrient concentration, $K_{\max}$ is maximum environmental capacity and I_{b0} is daily-averaged solar radiation under fair weather at river bed, respectively. The influence functions of solar radiation f_I, g_I, water temperature f_T and nutrient concentration f_N represent the effects of each environmental factor on specific growth and environmental capacity, and they are expected to take the value between 0 to 1.

The influence functions of solar radiation $f_I(I_b)$ and $g_I(I_{b0})$ were assumed to obey Monod type function;

$$f_I(I_b) = \frac{I_b}{I_{bc} + I_b}, \quad g_I(I_{b0}) = \frac{I_{b0}}{I_{b0c} + I_{b0}} \tag{4a, b}$$

in which I_{bc} and I_{b0c} are the half-saturated values of solar radiation. The influence function of water temperature was given by the following equation;

$$f_T(T) = \exp\left[\alpha_T \frac{(T - T_{opt})^2}{(T_c - T_{opt})^2}\right] \tag{5}$$

in which T_{opt} is the optimal water temperature for the growth of periphyton, α_T and T_c is the numerical parameters. The function for nutrient concentration f_N was modeled by Monod type function;

$$f_N(N) = \frac{N}{N_c + N} \tag{6}$$

in which N_c is the half-saturated value of nutrient concentration. The profiles of the influence functions are depicted in figure 2.

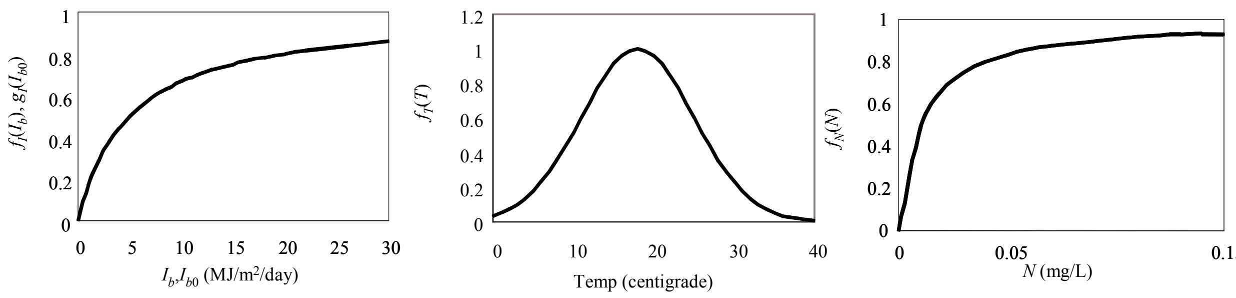

(a) Solar radiation　(b) Water temperature　(c) Nutrient concentration

Figure 2　Influence functions of solar radiation, water temperature and nutrient concentration

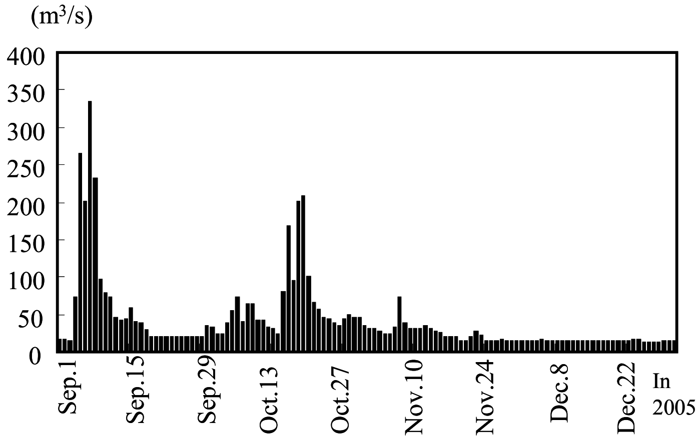

Figure 3 Hydrograph of the computational period

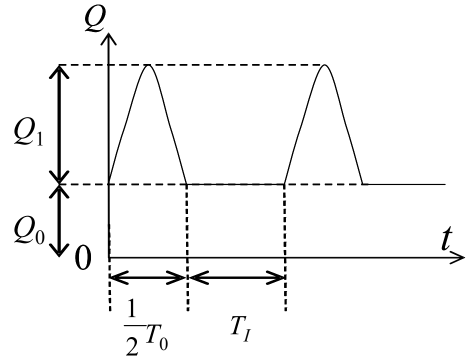

Figure 4 Discharge condition for various flood intervals

Table 1 Physiological parameters used in the present numerical simulation

Item	Value	Reference
μ_{max}	1.1 (day^{-1})	estimated from field data
K_{max}	38.4($mg.chl.a/m^2$)	estimated from field data
T_{opt}	18 (^oC)	Nozaki et al. (2003)
α_T	-2.3	Ikeda et al. (1998)
T_c	3(^oC)	Ikeda et al. (1998)
δ	0.05	assumed
λ	0.18(m^{-1})	assumed
I_c	5($MJm^{-2}day^{-1}$)	Tashiro (2004)
N_c	0.01(mg.N/l)	Nozaki et al. (2003)

2.3 Computational conditions

The computational conditions were given to the measurement values at the downstream reach of the Yahagi river in Japan. The computational domain was taken at a reach between 16.8 km and 17.6 km from the river mouth. The domain was divided into 20 grids in longitudinal direction and 22 grids in transverse direction. The numerical computation was performed under the hydrological and metrological conditions during September 1 and December 31, 2005. Figure 3 shows the hydrograph at the study site during the Sep. and Dec. in 2005. The downstream boundary condition for water level was given to the interpolated value calculated from the daily maximum water levels measured at 4 km downstream and 7.5 km upstream from the study site. The inlet water discharge was given to the discharge measured at the study site. The water temperature and the nutrient concentration during the computational period were given to the values measured at 7 km downstream from the study site.

In order to evaluate the effects of river discharge on periphyton growth, two series of the numerical computations were performed. One case is the increased discharge case, in which the inlet condition of river discharge is increased by the amount of 5, 10, 20, and 30 m^3/s to the discharge measured at the Yahagi river, respectively. The other case is for detecting the effects of flood frequency on periphyton growth, in which the artificial discharge pattern was

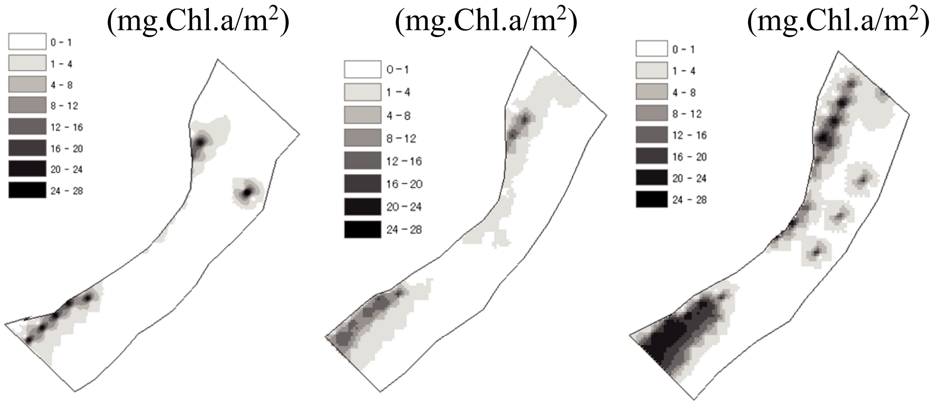

(1) Oct. 30 (2) Nov. 16 (3) Dec. 12

(a) Numerical simulation

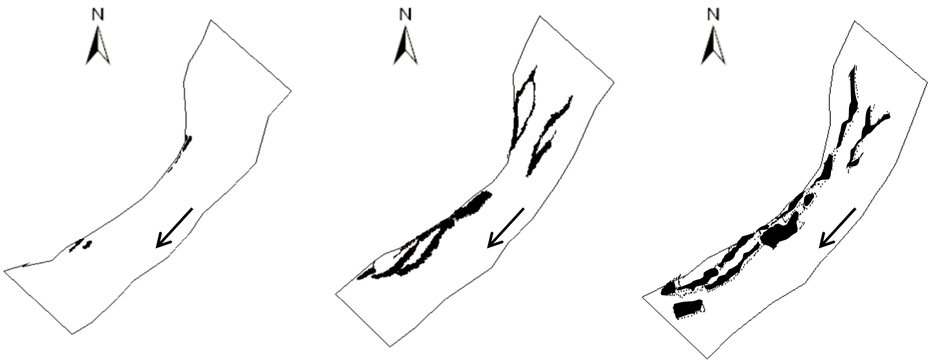

(1) Oct. 30 (2) Nov. 16 (3) Dec. 12

(b) Field measurement

Figure 5 Spatial distribution of periphyton biomass

supplied for the inlet condition (figure 4). The ordinary river discharge, Q_0, is set to be 30 m^3/s, and the peak discharge of flood, Q_0+Q_1, and the period of a flood, $1/2T_0$, are given to 130 m^3/s and 1 day, respectively. A series of the numerical simulation was performed under the different flood interval T_I (T_I= 1, 2, 4, 8, 16, 32, 64 and 128 days).

In the present computation, grain size of the bed material was set to be 1.0 mm, since the mean sand size at the periphyton growth area was about 1.0 mm. The Manning's roughness coefficient was given to 0.032 by calibrating the result of computation of flowing water area to that observed in the field. The physiological parameters used in the growth simulation for periphyton are summarized in table 1.

3. RESULTS OF THE NUMERICAL SIMULATION

3.1 Spatial Distribution of Periphyton Biomass

Figures 5 (a) represents the computational results of the spatial distributions of periphyton biomass, and the distributions of the periphyton measured at the Yahagi river are shown in figure 5 (b). The periphyton biomass computed tends to become large near the right

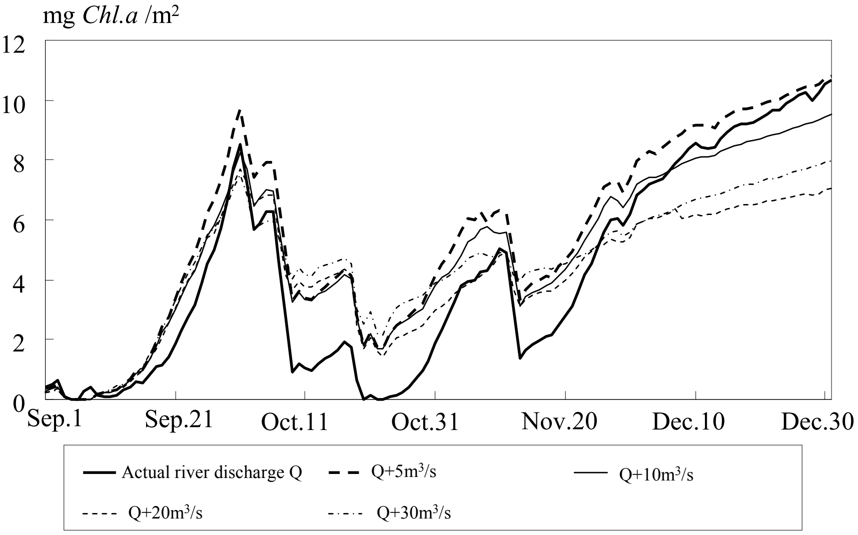

Figure 6 Time variation of biomass under the different discharge conditions

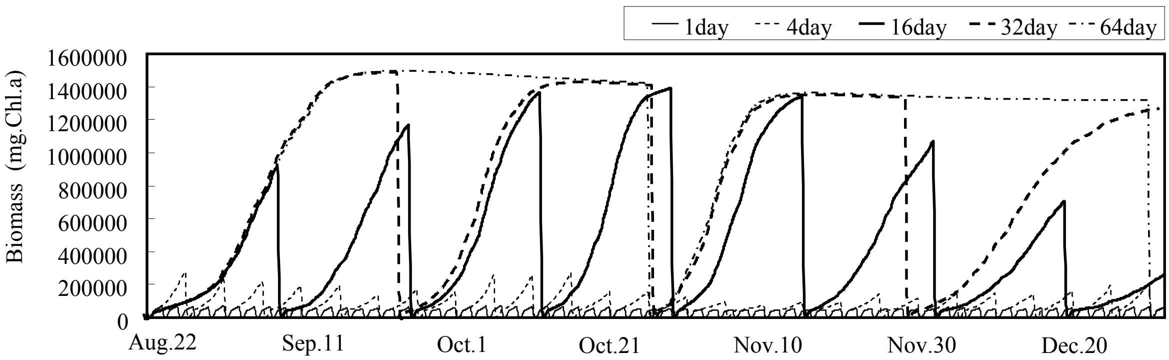

Figure 7 Time variation of biomass under the different flood intervals

side bank, and the growth area expanded from Nov. 16 to Dec. 12, and the results agree with the measurements in the field. Therefore the present computation can predict the growth of periphyton in the sand river well, and the growth and the spatial distribution of periphyton are closely correlated with the flow characteristics in sand rivers.

3.2 Effects of River Discharge on Periphyton Biomass and Primary Production

The time variations of the periphyton biomass under the different discharge conditions are illustrated in figure 6. The periphyton biomass was found to increase during late Sep. to middle Oct. and during late Oct. to the end of the computational period for all 5 cases, and, however, there was no clear trend of the response of the biomass to the increased discharge for 5 cases. Table 2 summarizes the averaged biomass and the averaged net primary production of periphyton, and the averaged biomass and the primary production vary with the increased discharge irregularly. If the geometry of river cross-section is rectangular, the bottom shear stress increases with river discharge, which decreases the growth of periphyton. However, the increased river discharge on the actual river geometry produces new shallow water area near the banks of the river, which provides the new suitable habitat for periphyton growth. Therefore, the simple increase of river discharge cannot suppress the growth of periphyton in actual rivers.

The time variations of periphyton biomass under the different flood intervals are

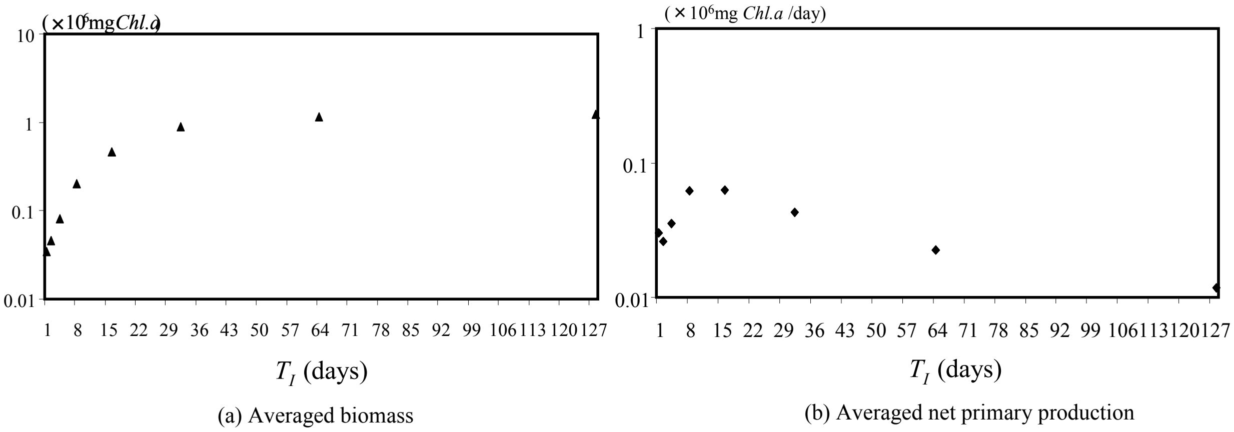

Figure 8 Response of periphyton biomass and primary production to the various flood intervals

shown in figure 7. The growth of periphyton increases with the flood intervals, and for the case that the flood interval longer than 32 days, the growth curve of the periphyton at each term reaches to the equilibrium periphyton biomass. The responses of the time averaged periphyton biomass and the amount of primary production to the various flood intervals are summarized in figures 8 (a) and (b), respectively. It was found that the time averaged periphyton biomass increases with the flood interval. On the other hand, the net primary production of periphyton takes a peak values at the flood interval ranging about 8 to 16 days. The high frequency of floods destroys the periphyton communities every turn, which prohibits the large growth of periphyton, resulting both the small biomass and primary production for high flood frequency. As the interval of floods becomes longer, the biomass per unit area of periphyton increases in accordance with the logistic equation, which yields the larger primary production. However, the further increase of flood interval reduces the renewal of the periphyton communities, and the biomass of periphyton tends to approach to the equilibrium environmental capacity. At this moment, net primary production approaches to zero, and the primary production, therefore, becomes small value at the large interval of floods.

4. CONCLUSIONS

In the present study, the numerical simulation was presented to describe the growth characteristics and the primary productivities of stream periphyton in a sand river. The results of the numerical simulation have revealed the followings:

The growth of periphyton at sand rivers was closely associated with the flow characteristics of the river, and the numerical simulation model combining the flow computation and the growth simulation of periphyton can estimate the spatial distribution of periphyton biomass in sand river well.

While the time averaged periphyton biomass increased with the flood interval, the net primary production of periphyton takes a peak value at the flood interval ranging about 8 to 16 days.

ACKNOWLEDGMENTS

The present study has been financially supported by the Special Coordination Funds for Promoting Science and Technology, Ministry of Education, Culture, Sports, Science and

Technology.

REFERENCES

Ikeda, S., Toda, Y. and Sano, T. 1998. Study on hydraulic characteristics and production rate of chlorophyll-a at riffles by field observation, *Journal of Hydraulic, Coastal and Environmental Engineering*, JSCE, 593, 93-104. (in Japanese)

Iwagaki, Y. 1956. Hydrodynamic study on critical bed shear stress, *Transactions of the Japan Society of Civil Engineers*, JSCE, 41, 1-21. (in Japanese)

MacIntire, C. D. 1973. Periphyton dynamics in laboratory streams: a simulation model and its implications, *Ecological Monograph*, 43, 399-420.

Minshall, G. W. 1978. Autrotrophy in streams, *Bioscience*, 28, 767-771.

Nozaki, K., Kohmatsu, Y., Yamamoto, T., Goto, N. and Mitamura, O. 2003. Photosynthetic activity of a filamentous green alga *Cladophora glomerata* in the middle region of the Yahagi River, *Report of Yahagi River Institute*, 7, 169-173. (in Japanese)

Saravia, L. A., Momo, F. and Lissin, L. D. B. 1998. Modeling periphyton dynamics in running water, *Ecological Modeling.*, 114, 35-47.

Tashiro, T. 2004. *Study on Evaluation of Aquatic Ecosystem in a Stream with Less Disturbance after Dam Construction*, Doctoral Thesis, Nagoya University. (in Japanese)